PRELIMINARY SHEAR WAVE SPLITTING INVERSION RESULTS FOR PUNA GEOTHERMAL FIELD

A. Lucas, E. Shalev & P. Malin

Institute of Earth Science and Engineering, 58 Symonds St, Private Bag 92019, Auckland, Aotearoa–New Zealand

a.lucas@auckland.ac.nz

Keywords: *Shear wave splitting, Inversion*

ABSTRACT

A new method of linear inversion for sub-surface crack density is presented. The method is based on shear wave splitting (SWS) observations (time delay and polarization angle) which are a direct measure of the shear wave velocity anisotropy analogical to birefringence in optics. The relationship between crack density and SWS observations is non-linear. By fixing the crack dip to vertical and the strike to the SWS polarization angle the relationship becomes approximately linear and can be solved using LSQR. By including observations where the earthquake does not display SWS, the inversion is further constrained thus improving the resolution. A crack density inversion is calculated for a large (~9500) data set of earthquakes detected at the Puna geothermal field. This data is detected by a local seismic array consisting of eight borehole seismometers. Results indicate that there is a large area of high crack density in the south of the field. The results also indicate two linear features (one of which correlates well with drilling records) in the shallow (1.8km) regions of the field.

1. INTRODUCTION

1.1 Geological setting

The Puna area is located in the Kilauea Volcano East Rift Zone (KERZ), Big Island, Hawaii. The rift is locally defined by a combination of fissure eruption craters and normal faulting, both of which strike in the same NE-SW trend as the rift (**Figure 1**). The rift has been volcanically active in the recent past (last eruption 1960) and the resulting lava flows have resurfaced the area obscuring all fault activity predating the lava. In the Puna area the rift makes a small (approximately 1km) left step (looking along strike) with no observed corresponding transverse faulting (**Moore and Trusdell (1991)**). In the area of the step the Puna Geothermal Venture Co (PGV) has established a geothermal power station. The PGV lease boundary is displayed in **Figure 1**; this is used as a reference point for this paper. Drilling data provided by PGV indicate that production is concentrated in the southern part of the lease. These data also indicate a major fault system trending NE in the southern section of the lease.

1.2 The seismic network

The seismic network in Puna was established in 2006 and consists of eight stations. Of these eight stations, five are 2-Hz and three are 4.5-Hz geophones. The geophones are installed in boreholes varying in depth from 24-210 m. Data are continuously recorded at a sampling rate of 200 sample/sec. They are then analyzed using a triggering algorithm to generate trigger files which are then manually picked. This allows the location of all picked earthquakes using Hypoinverse (**Klein (2012)**). The magnitudes are calculated using the moment method (**Andrews (1986)**) and are calibrated using earthquakes co-located by the Hawaiian Geothermal Observatory. This calibration showed that the lower detection limit for the network is -0.2 moment magnitude.

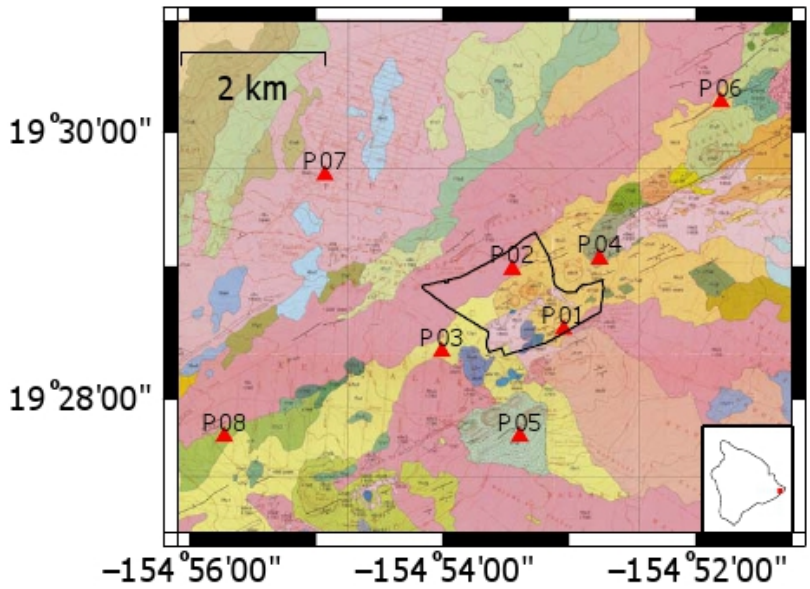

Figure 1: Geological map of the Puna area with seismic stations and PGV lease boundary added. The PGV lease boundary has been added to use as a reference in all figures in this paper. Background map: Moore and Trusdell (1991).

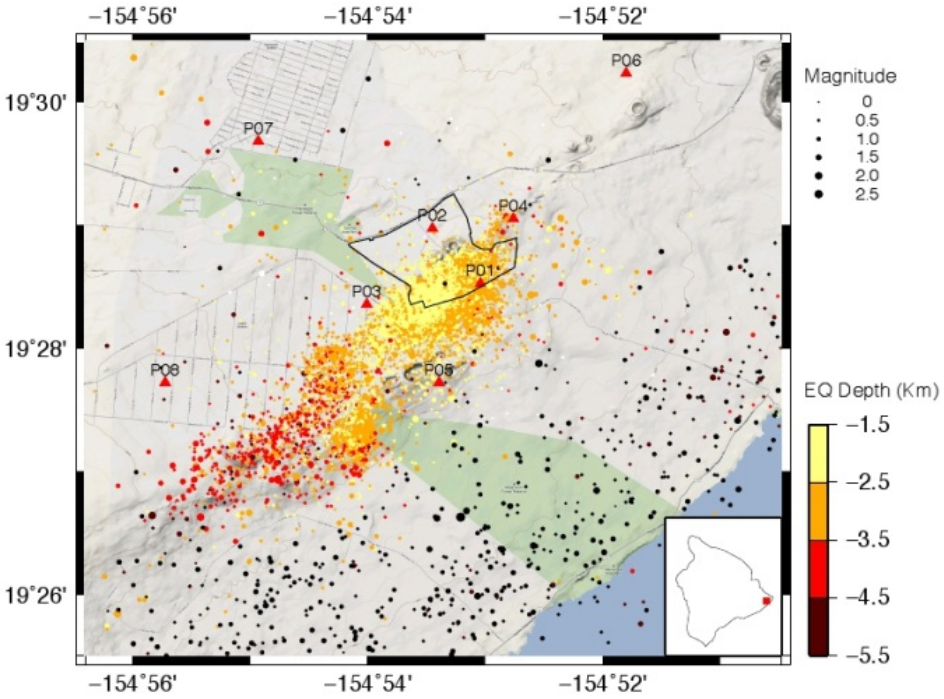

Figure 2: The seismicity detected by the PGV seismic array in the Puna area.

A total of 9562 earthquakes have been detected in and around the Puna area. The seismic network was installed after the commencement of production. Therefore it is not clear how much of the seismicity is due to production and how much is natural. The location of these earthquakes follows the rift trend in a NE-SW direction, however to the NE of the step the rift becomes aseismic (**Figure 2**). In the area of the step the seismicity is both densest and shallowest.

1.3 Introduction to shear wave splitting

In seismology shear wave splitting (SWS) is the measure of seismic velocity anisotropy analogical to birefringence in optics. It presents in earthquake traces as two shear wave arrivals separated by a small (of the order of 0.1s) delay in time (Crampin and Peacock (2008)). The polarization of these arrivals is often (althrough not always) orthogonal to each other and the P-wave particle motion (Figure 3a). In the crust seismic anisotropy has two proposed causes, parallel aligned fracture systems (Anderson et al (1974)), and lattice preferred orientation (Silver and Chan (1991)), with the dominate effect in the upper crust assumed to be parallel fractures (Crampin (1994))

.

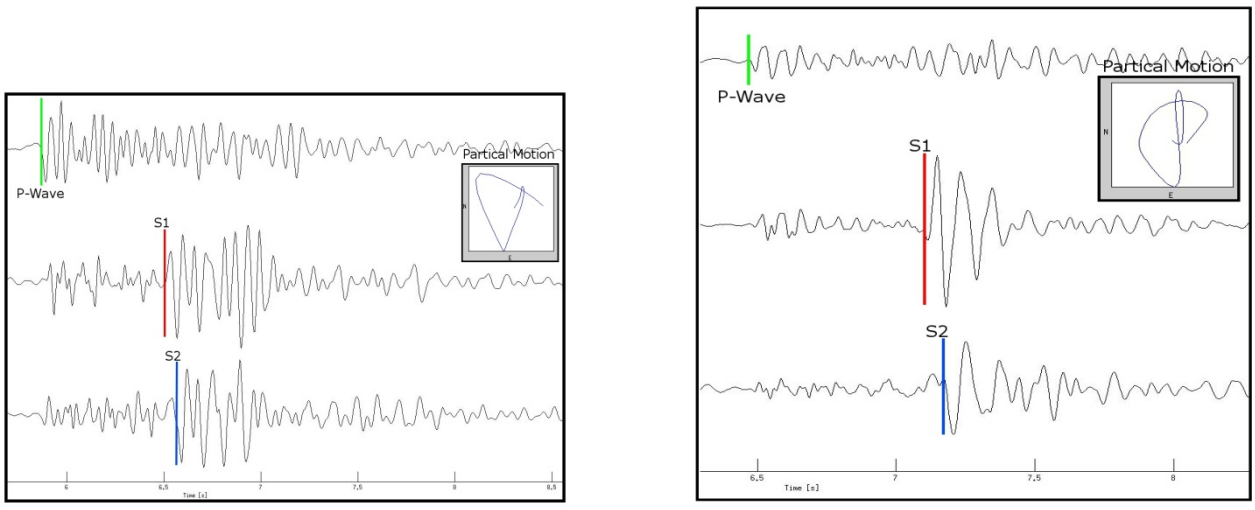

Figure 3a (upper) and 3b (lower): Examples of SWS observed at Puna. The traces have been rotated so that the top trace is along P-wave polarization direction and the two below are orthogonal. The picked split shear waves are indicated as S1 (red) and S2 (blue) as well as the P-wave (green). The particle motion of the two orthogonal traces (from a small window around the two S-wave picks) is displayed in a small window in the top right corner.

The fracture system generating any measured SWS must occur at some point along the path of shear wave propagation between earthquake and station. Immediately before entering the area of fracture based anisotropy the shear wave is polarized in a direction related to the focal mechanism of the earthquake. Upon entering, the wave splits into two discrete waveforms due to the velocity anisotropy caused by the fractures. The shear wave velocity is fastest parallel to the fractures and slowest perpendicular, resulting in shear waves polarized parallel and perpendicular to fracture strike. This velocity anisotropy also results in each wave experiencing a different velocity, therefore the more time they spend in the fractured area the larger the time delay between the two wave forms. When the waves exit the fracture zone they both experience the same velocity and thus propagate in the same manner but as separate waves.

For the purposes of analyzing the fracture systems that generate SWS a quantity called crack density is defined as:

$$\varepsilon = \frac{n}{v}a^3 \quad (1)$$

Where each crack is assumed to be a thin water filled disk with radius a, n is the number of cracks in a unit volume v and the crack density is ε (**Hudson (1981)**). The radius a is required to be significantly less than the wavelength of the S-wave, which is the case in most scenarios. It is seen that ε is a unit less, non-negative quantity and that $\varepsilon = 0$ represents unfractured rock. From **Hudson (1981)** and **Sato et al (1991)** two shear wave velocities can be derived for a given crack density ε :

$$V_p^2 = \beta^2\left\{1 - \frac{8}{7}\varepsilon(1 + cos4\theta)\right\} \quad (2)$$

And

$$V_r^2 = \beta^2\left\{1 - \frac{8}{7}\varepsilon(1 + cos2\theta)\right\} \quad (3)$$

The velocities V_p and V_r are for shear waves polarized parallel and perpendicular to the cracks respectively, β is the shear wave velocity of the same rock without fractures and θ is the angle between the direction of the propagating wave and a normal to plane of the fractures. By a first order Taylor series approximation an equation relating the crack density to the SWS time delay τ can be derived:

$$\tau = \frac{4\varepsilon}{7\beta}(cos4\theta - cos2\theta)R \quad (4)$$

Where R is the propagation distance inside the zone of fracture based anisotropy. From this equation it can be seen that the time delay observed is a function of both the angle of incidence and the crack density. It also important to note that in this relationship τ is positive for $60^\circ < \theta < 90^\circ$ and negative for $0 < \theta < 60^\circ$, i.e. for angles of incidence below 60° the observed fast polarization direction is perpendicular to that above 60°.

2. SWS IN GEOTHERMAL SYSTEMS

SWS is commonly used in large scale studies (**Abt and Fischer (2008)**), it is less often applied to small scale arrays such as those used to detect micro-seismicity in geothermal systems. However studies in Krafla (Iceland) (**Chuanhai et al (2008)**), Geysers (California) (**Elkibbi and Rial (2005)**) and Coso (California) (**Rial et al (2005)**) show SWS is not uncommon in these geothermal areas. The results of these studies show varying degrees of correlation with known production features. Analysis of the results consists of comparing station polarization angles to known fault orientations. Inversions of data focus on two methods of dealing with the non-linearity of **equation 4**; either a set of assumptions are made about the fracture orientation (**Shalev and Lou (1995)** and **Lou and Rial (1997)**) or an iterative non-linear approach is used (**Yang et al (2005)**).

3. PICKING SWS ARRIVALS

Currently all automated picking techniques for identifying separating and picking SWS arrivals present inaccuracies. Most techniques fall into two broad groups: cross-correlation techniques or linearity techniques (**Crampin and Gao (2006)**). In both techniques the three component earthquake trace is first rotated so one component is parallel to the P-wave polarization direction and the other two are orthogonal.

To automatically identify and pick SWS arrivals at Puna a combination of both methods has been used. A range of window lengths starting at a range of times around the manual S-wave pick are generated. For each of these windows the polarization angle is calculated from a short subsection at the beginning of the window and given a penalty of the linearity (lin_{S1}) (**Aster et al (1990)**). The two traces are then rotated to this angle and the cross-correlation calculated. This gives a time delay at the maximum of the absolute of the cross-correlation between the two traces and a penalty of the cross-correlation value ($corr_{S1-S2}$). The linearity of the second arrival (lin_{S2}) and the sine of the angular difference between the two polarizations ($\theta_{S1} - \theta_{S2}$) are also calculated for each window. The total penalty for each window is calculated using the formula:

$$Pen_{win} = lin_{S1}\, corr_{S1-S2}\sqrt{lin_{S2}}\sqrt{\sin(\theta_{S1} - \theta_{S2})} \quad (5)$$

Each of the components in Pen_{win} varies between 0 and a perfect SWS penalty of 1, therefore Pen_{win} also maximizes at 1. The square root in $\sqrt{lin_{S2}}$ and $\sqrt{\sin(\theta_{S1} - \theta_{S2})}$ down weights them in comparison to the other components of Pen_{win}. This is done as the slow S-wave arrival is more likely to be contaminated by interfering signals. If the window with the highest Pen_{win} is above a user specified threshold then the time delay and polarization are stored as a SWS observation. If all windows are below the user specified value then the earthquake-station pair is stored as not displaying identifiable SWS. Testing has shown this picking technique to be moderately accurate, high quality SWS observations are well identified, however an amount of noise is often present. Currently work is progressing on the development of a better automated picker.

4. INVERSION TECHNIQUE

Any inverse problem can be described by the matrix equation:

$$\boldsymbol{A}x = d$$

The crack density model being solved for is the vector x and the data that is being used to solve for the model is the vector d. Each observation of SWS (for a station-earthquake pair) is counted as a single value of d. The matrix $\boldsymbol{A}$ contains the physical relationship between the model and the data. If the relationship is linear, existing techniques (such as LSQR) are used to solve for x.

We present a new method of inverting for crack density, this method contains a number of improvements from the method outlined in **Shalev and Lou (1995)**. In this new method it is assumed that all SWS present is generated through fracture anisotropy and obeys the relationship in **equation (4)**. As this relationship is non-linear due to the dependence on the angle of incidence between the shear wave propagation direction and fractures, some assumptions need to be made to linearize it. We first assume that all fractures present have a vertical dip, secondly we assume the strike of the fractures does not vary along the earthquake-station path and is defined at the beginning of the inversion. There are two methods of defining the strike angle: forcing all fractures in the inversion domain to have the same user defined strike taken from geological mapping; or to use the polarization angle of the S-wave identified at picking as the strike. Each of these techniques has benefits and drawbacks. Current testing has shown that the two methods produce similar inversion results with small scale differences in the inversion result. For the purposes of this paper all inversion results are calculated using picked polarization angles as the fracture strike for each observation.

The crack density model (x) is parameterized using a linear grid of voxel locations for which the crack densities need to be determined. This parameterization allows the transfer of the model from a 3D grid to a vector of node locations. It is assumed that SWS anisotropy is a small magnitude effect overwritten on the bulk shear wave velocity, and the ray approximation of the wave equation is applicable i.e. the volumes of homogeneous fracturing being investigated are larger than or of the order of the wavelength of the S-waves. Thus the anisotropy causes little deviation from that of a ray propagating through the same isotropic medium. This allows the tracing of all rays from their earthquake sources (through a 3D velocity model generated using the method of **Shalev and Lees (1998)**) to the corresponding station identifying which nodes each ray transits. The tracing is done through the commonly used method of ray bending (**Nolet (2008)**). This allows the forming of the matrix $\boldsymbol{A}$ through:

$$\boldsymbol{A(o,n)} = \frac{\boldsymbol{4R(o,n)}}{\boldsymbol{7\beta(o,n)}}(\boldsymbol{cos4\theta(o,n)} - \boldsymbol{cos2\theta(o,n)})$$

Where o is the observation number and n is the node number. At each node the incident angle on vertical fractures ($\theta(o,n)$) and the length of the ray, inside the node ($R(o,n)$) are calculated. Due to the Earths velocity structure the ray tends to become more vertical as it moves to the surface. Thus the angle $\theta(o,n)$ changes along the ray path even through the strike of the fractures is fixed. Most inversion techniques only use rays from earthquakes which fall within a 40° cone from the vertical at the station (**Crampin and Peacock (2008)**). We propose a different criterion: only using rays which have an incidence at the surface of within $10^{\circ} - 15^{\circ}$of the vertical. This allows the inclusion of slightly more earthquakes which are outside the old criteria. It also removes the possibility of the SWS being incorrectly identified due to surface effects such as converted waves. In this paper the angle of incidence is measured by ray tracing, however it is also possible to measure this from the P-wave particle motion.

In inversions it is possible to weight each observation by the confidence in which it is held. In this inversion each SWS observation is weighted by a combination of the quality of the pick and the length of the ray. The ray length is included because a short ray displaying SWS has a higher degree of confidence that the area of fracturing occurs at some point along the ray path.

It is possible to calculate an inversion result using only the picked SWS observations. However it also can be stated that rays (null rays) which fulfill the geometric criterion (inside the $10^{\circ} - 15^{\circ}$ incident angle) to be included in the inversion and do not show SWS are an observation. We propose to include these observations by giving them a time delay of the order of the error in time delay picking and a polarization angle set as the average of all picked SWS observations. The null rays then can be passed through the same ray tracing process as the rays displaying SWS and added to the inversion framework. The weights of all the null rays are set to the minimum quality of the SWS observations. Adding the null rays to the inversion frame work has been found to increase the resolution of the result.

Most geophysical inversions are approximately linear and thus the starting model has a high degree of influence. We use a homogeneous starting model with a user-input value. This means the inversion needs run multiple times to find a suitable starting model which results in a low starting model misfit from the observed data. Once the matrix $\boldsymbol{A}$ is formed and the model parameterized the inversion is solved by the classic LSQR method.

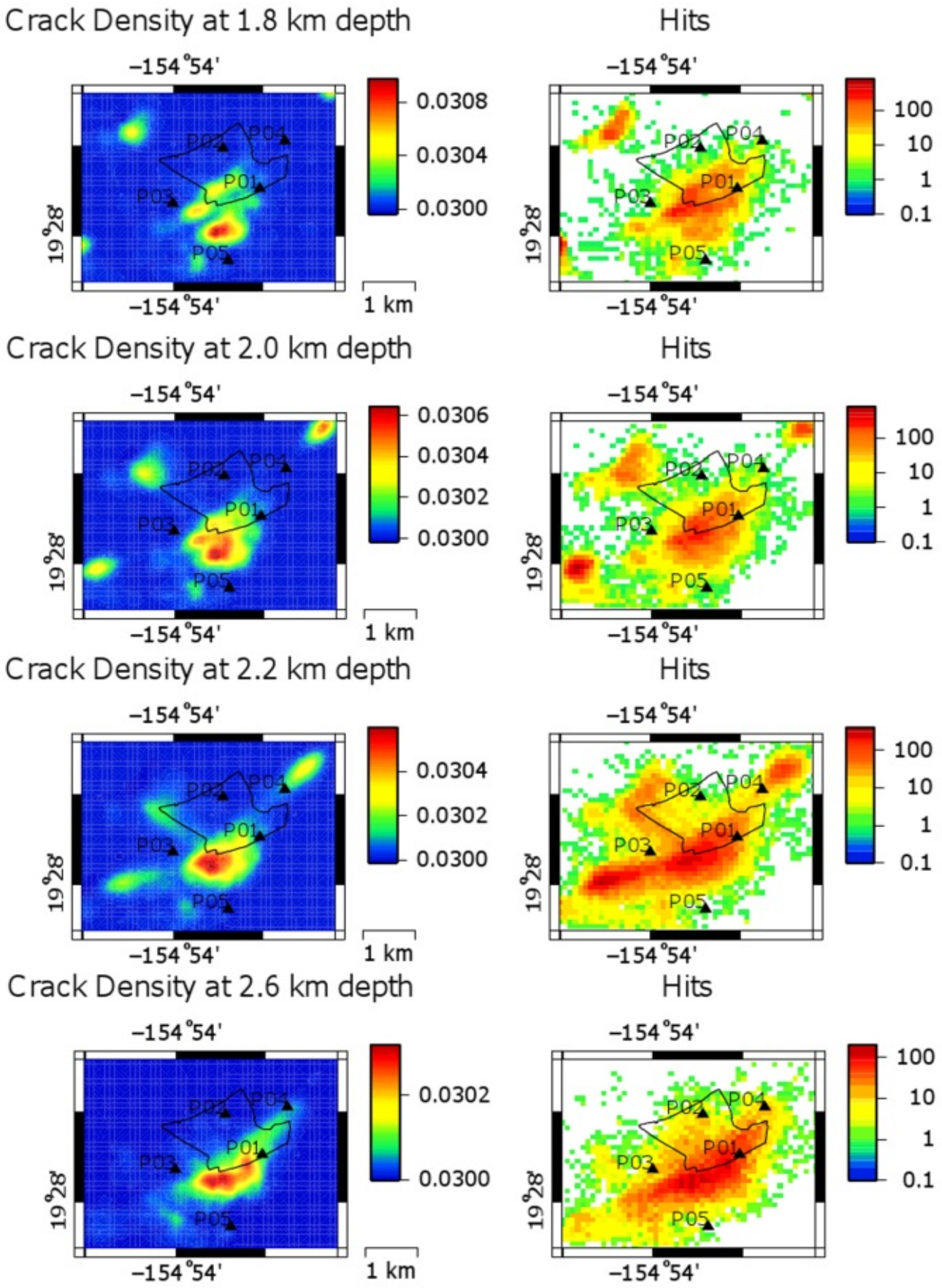

Figure 3: SWS inversion results for Puna geothermal system. The plots on the left are depth slices of the inversion results and on the right are the corresponding total hit plots. On each plot, the stations and PGV lease are displayed for reference. Note: the color scales vary with depth and both scales are unit less numbers.

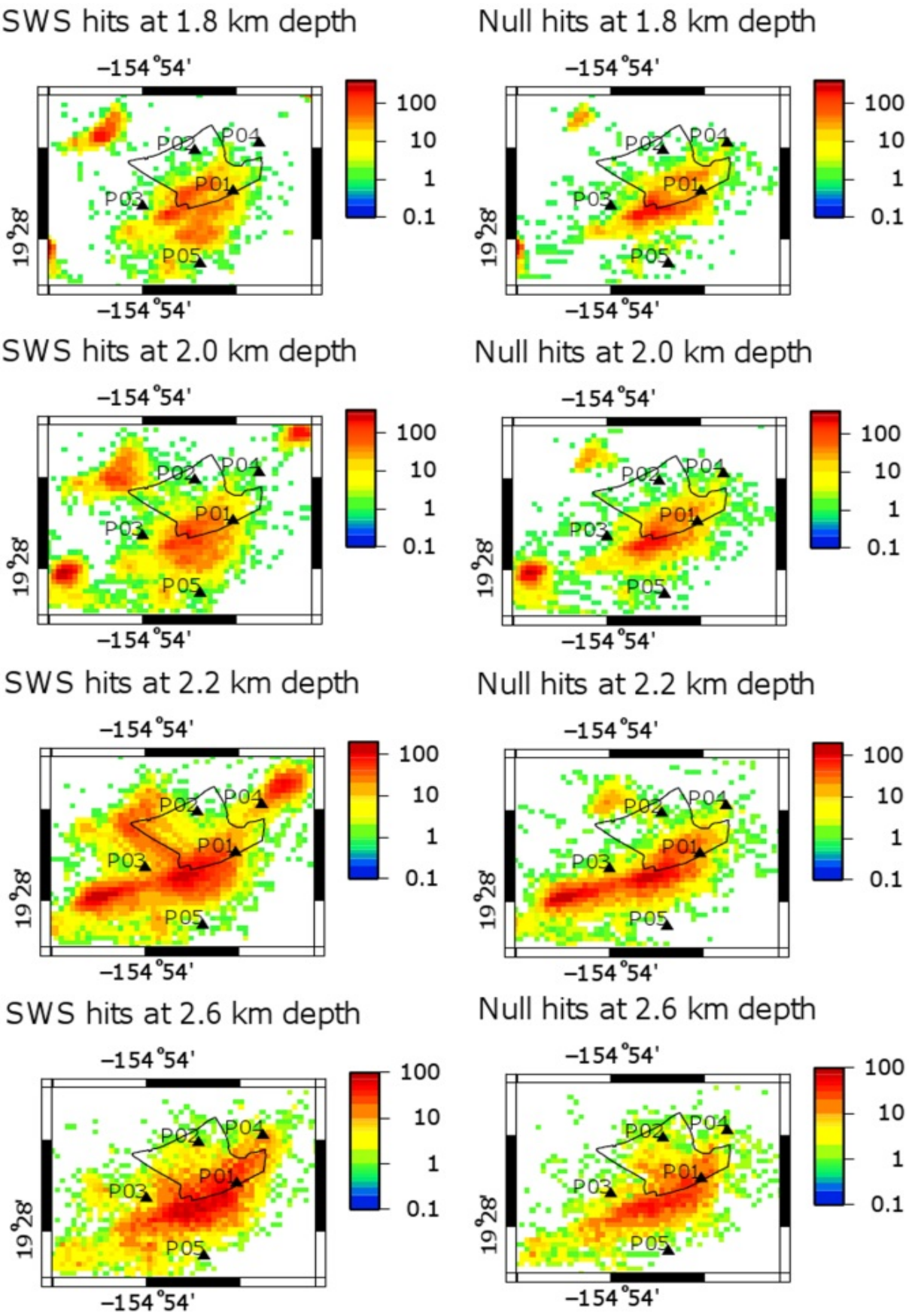

Figure 4: Hit plots for Puna geothermal system. The plots on the left are depth slices showing the nodes are transited by rays displaying SWS, the plots on the right are nodes which rays <u>not</u> displaying SWS transit. On each plot, the stations and PGV lease are displayed for reference. Note: the color scales vary with depth and both scales are unit less numbers.

5. RESULTS

Of the 9562 earthquakes registered by 8 stations at Puna 21741 earthquake-station pairs were found to have SWS using the picking technique discussed in this paper. There are clear cases of SWS in the waveforms observed, see **Figures 3a** and **3b**. A further 14853 earthquake-station pairs were found to satisfy the inversion conditions for SWS (were inside the $10^{\circ} - 15^{\circ}$ incident angle) but had no splitting (null rays).

Crack density inversion results, as shown in **Figure 4** left column, indicate that anisotropy is present at Puna. The ray coverage however is very low or non-existent in some areas (see **Figure 4** right column) due to the earthquake and station distribution (**Figure 2**). The only area of high confidence in the inversion result is in the SE of the lease area. The distribution also results in some inversion artifacts between the earthquake cloud and the distant stations. It is highly unlikely that these artifacts represent a real crack density at their locations.

In the crack density results at 1.8 km depth, a linear feature trending NE is seen in the same location that drilling data indicates a fracture zone. A second feature is also seen to the south of the lease boundary. These two features form a singular crack density high at depth until the earthquake distribution drops off with depth around 2.4 km. However due to the distribution of earthquakes and stations confidence in these results is only moderate. Preliminary jackknife testing indicates a moderate degree of stability (and thus confidence) in these results, however further testing is required to confirm the results and due to time constraints they not available for this paper.

The distribution of ray paths for rays showing SWS (**Figure 5** left column) as compared to those not showing clear SWS (**Figure 5** right column) show some similarities and differences. This is not unexpected as the noise present in the picking of SWS arrivals causes some degree of overlap between the two types of observation, the best way to improve on this is to improve picking techniques. The inversion technique deals with this by identifying the overlying trend in the data. At 1.8 km the rays showing SWS appear to maximize in a different pattern. With depth the differences become less pronounced, however it is clear that the rays traveling to the NW displaying SWS travel along a very different path to those without. If the inversion is calculated with out the improvements mentioned in this paper these details are less apparent.

6. CONCLUSION

A new method is presented of inverting for a crack density distribution using shear wave splitting (SWS) observations. This inversion includes improvements such as parameters which vary along the ray path and the inclusion of rays which do not display SWS. The inversion results for Puna display a linear feature correlating with existing geological models. A high in crack density is also seen at depth in the southern area of the inversion volume.

ACKNOWLEDGEMENTS

The assistance of Puna Geothermal Venture Co in providing access to the data required for this paper is appreciated by the authors. Without the long term assistance of companies such as this the research presented here would not be possible.

REFERENCES:

Anderson, D. L., Minster, B. and Cole D.: *The effect of oriented cracks on seismic velocities.* Journal of Geophysical Research, vol 79, no 26, pp 4011-4015, (1974).

Andrews, D. J.: *Objective determination of source parameters and similarity of earthquakes of different size*. Earthquake Source Mechanics, pp 259-267, (1986).

Abt, D.L. and Fischer K.M.: *Resolving three-dimensional anisotropy structure with shear wave splitting tomography*. Geophysics Journal International, vol 173, pp 859-886, (2008).

Aster, R. C., Shearer, P.M. and Berger J.: *Quantitative measurements of shear wave polarizations at the anza seismic network, southern California: implications for shear wave splitting and earthquake prediction.* Journal of Geophysical Research, vol 75, no B8, pp 12449-12473, (1990).

Chuanhai T., Rial J.A. and Lees J.M.: *Seismic imaging of the geothermal field at Krafla, Iceland using shear-wave splitting.* Journal of Volcanology and Geothermal Reasearch, vol 176, pp 315-324, (2008).

Crampin S.: *The fracture criticality of crustal rocks.* Geophyisics Journal International, vol 118, pp 428-438, (1994).

Crampin S. and Gao Y.: *A review of techniques for measuring shear-wave splitting above small earthquakes.* Physics of the Earth and Planetary Interiors, vol 159, pp 1-14, (2006).

Crampin S. and Peacock S.: *A review of the current understanding of seismic shear-wave splitting in the earths crust and common fallacies in interpretation.* ,Wave Motion vol 45, pp 675-722, (2008).

Elkibbi M. and Rial J.A.: *The Geysers geothermal field: results from shear-wave splitting analysis in a fractured reservoir.* Geophysics Journal International, vol 162, pp 1024-1035, (2005).

Hudson J.A.: *Wave speeds and attenuation of elastic waves in material containing cracks.* Geophyisics Journal of the royal astronomical society, vol 64, pp 133-150, (1981).

Klein F.W.: *Users guide to HYPOINVERSE-2000, a fortran program to solve for earthquake locations and magnitudes.* USGS open file report 02-171 revised, V1.37, (2012).

Lou M. and Rial J.A.: *Characterization of geothermal reservoir crack patterns using shear-wave splitting.* Geophysics, vol 62, no 2, pp 487-494, (1997).

Lou M., Shalev E. and Malin P.E.: *Shear-wave splitting and fracture alignments at the northwest geysers, California*. Geophysical Research Letters, vol 24, no 5, pp 1895-1898, (1997).

Moore, R.B. and Trusdell, F.A.: *Geologic map of the lower east rift zone of Kilauea Volcano, Hawaii* U.S.

Geological Survey Series and Number: Miscellaneous Geologic Investigations Map I-2225, (1991).

Nolet, G.: *A breviary of seismic tomography imaging the interior of the earth and sun.* Cambridge University Press, (2008).

Rial, J.A., Elkibbi M. and Yang M.: *Shear-wave splitting as a toolfor the characterization of geothermal fracture reservoirs: lessons learned* Geothermics, vol 34, pp 365-385, (2005).

Shalev, E. and Lees J.M.: *Cubic B-splines tomography at Loma Prieta.* Bulletin of the seismological society of America, vol 88, pp 256-269, (1998).

Shalev, E. and Lou M.: *A preliminary tomographic inversion of crack density in the Coso geothermal field.* EOS (Transactions), vol 76, no 46, pp 351, (1995).

Sato, M., Matsumoto N. and Niitsuma H..: *Evaluation of geothermal reservoir cracks by shear-wave splitting of acoustic emission.* Geothermics, vol 20, no 4, pp 197-206, (1991).

Silver, P. G. and Chan W.W.: *Shear wave splitting and subcontinental mantle deformation.* Journal of Geophysical Research, vol 76, no B10, pp 16429-16454, (1991).

Yang, M., Elkibbi M. and Rial J.A.: *An inversion scheme to model subsurface fracture systems using shear wave splitting polarization and delay time observations simultaneously.* Geophysics Journal International, vol 160, pp 939-947, (2005).